Geophys. J. ht. (1991) 104, 611-623

Wave propagation through fluid-filled inclusions of various shapes: interpretation of extensive-dilatancy anisotropy

Stuart Crampin
Edinburgh Anisotropy Project, British Geological Survey, Murchison House, West Mains Road, Edinburgh EH9 3LA, *UK*

Accepted 1990 October 16. Received 1990 July 24; in original form 1990 May 16

SUMMARY

Previous examinations of the effects of extensive-dilatancy anisotropy (EDA) on seismic waves have been largely restricted to discussions of parallel fluid-filled cracks of small aspect ratio. It is recognized, however, that EDA may be caused by stress-aligned fluid-filled cracks, microcracks, and preferentially oriented pore-space, in a variety of shapes, dimensions, and distributions, which may not be adequately modelled by the effects of uniform distributions of thin parallel cracks. The effects on seismic waves are examined for distributions of inclusions ranging from spherical pores and oblate spheroids (bubbles), to penny-shaped cracks. Unlike thin cracks, distributions of aligned oblate spheroids induce significant P-wave velocity anisotropy. In contrast, the parallel polarizations of the leading split shear waves within the shear wave window, which is one of the most distinctive features of shear waves in the crust, are preserved for all aspect ratios except spherical bubbles. The 3-D effects show minor variations that are most distinctive at small aspect ratios. Shear waves are very sensitive to changes in the geometry of such thin inclusions, and there is some observational evidence for temporal variations in splitting as the stress acting on the rockmass changes. If this sensitivity is confirmed it would suggest that the detailed geometry of a reservoir during production or enhanced oil recovery (EOR) might be monitored by repeated shear-wave VSPs.

Key words: EDA cracks, fluid-filled inclusions, varying aspect ratios.

1 INTRODUCTION

Shear wave splitting, diagnostic of effective seismic anisotropy, is almost universally observed in the uppermost 10–20 km of the Earth's crust (Crampin 1987). The splitting is caused by propagation through the distributions of stress-aligned fluid-filled inclusions known as extensive-***dilatancy anisotropy*** or ***EDA*** (Crampin, Evans & Atkinson 1984; Crampin 1987). The individual inclusions are known as ***EDA cracks*** because many of the effects may be modelled by distributions of flat penny-shaped microcracks, although in ***in situ*** rock the inclusions may include a wide range of shapes from flat cracks to oblate spheroids.

Fluid-filled inclusions are known to exist in most ***in situ*** rocks (Fyfe, Price & Thompson 1978). Since they are the most compliant elements of the rockmass, it is expected, and observations of shear-wave splitting confirm (Crampin 1987), that EDA cracks are aligned, like hydraulic fractures (Hubbert & Willis 1957), normal to the direction of minimum compression. EDA cracks in ***in situ*** rock are usually aligned parallel and vertical, since the minimum compressional stress is usually horizontal once below the anomalies associated with the near-surface stress and topographic irregularities (Crampin 1990).

Although it has been recognized that the candidate inclusions EDA may include a wide range of shapes and dimensions (cracks, microcracks, and preferentially oriented pore-space), the detailed discussions and numerical modelling to date have been largely restricted to distributions of parallel cracks of small aspect ratio (Crampin 1984, 1985). Such modelling may be inadequate to treat both the irregular intergranular pore-space expected in many sedimentary rocks and the nearly spheroidal pores that are commonly present in mineral crystals (Shepherd 1990). (We shall refer to as such nearly spheroidal pores as ***bubbles.)*** In some circumstances, bubbles might form a significant proportion of the fluid-filled inclusions in igneous and metamorphic rocks in the crust, and it is grains of such igneous and metamorphic rocks which are the constituent particles of many sedimentary rocks.

Douma (1988) examined distributions of cracks with aspect ratios up to ***AR*** = 1.0, but the velocity variations

were plotted as separate planar sections for each of the split shear waves. Interpretation of shear-wave splitting depends on identifying the spatial patterns of three critical parameters: (1) the polarizations of the leading (faster) split shear wave; (2) the time delay (velocity difference) between the split shear waves; and (3) the contact points of the two shear wave velocity surfaces (in point-, kiss-, and line-singularities, Crampin 1989). Information about these parameters cannot easily be obtained from Douma's separate plots of velocity variations.

[Note also that Douma uses the average density $\rho_a = (1 - \phi)\rho_m + \phi\rho_f$ of the solid, inclusive of the inclusions, to calculate the seismic velocities, where ρ_m and ρ_f are the densities of the matrix rock and the pore fluid, respectively, and ϕ is the volume concentration of the inclusions. He uses effective elastic constants obtained by various applications of the technique of Eshelby (1957), and modifying the density in this ***ad hoc*** way is not necessarily correct, any more than the average rigidity, say, gives a good estimate of the effective rigidity (J. A. Hudson, private communication). Eshelby's calculations were for a static system in which density plays no role, and the expressions for the effective parameters derived for these techniques can be used as a low-frequency approximation. Thus, the correct first-order approximation for density in calculations of the velocities of low-frequency waves (wavelengths much larger than the crack dimensions) through low-density cracks is the value of density in the matrix rock. The correct density used to obtain seismic velocities through rock with distributions of aligned inclusions of high porosity has not yet been investigated, but the effect is likely to be frequency dependent.]

Douma & Crampin (1990) examine the effects of changes in aspect ratio on (particularly) shear-wave particle displacements. This paper, is a systematic examination of the effects on the three parameters (polarizations, time delays, and singularities) of distributions of preferentially aligned water-filled inclusions of different shapes to find out what information about the properties of the inclusions can be inferred from the behaviour of seismic waves. The paper presents numerical models of the properties of seismic waves propagating through uniform distributions of a variety of inclusions ranging from flat penny-shaped cracks to shperes and oblate spheroids (bubbles), and through mixtures of cracks and bubbles.

Note that the expressions used to refer to waves in anisotropic rocks have been defined in Crampin (1989), and will not be repeated here.

2 MODELLING FORMULATIONS

Hudson (1980, 1981) used Eshelby's (1957) technique for calculating the effects on seismic waves of scattering at ellipsoidal inclusions. Hudson developed algebraic formulae for the first- and second-order effects on elastic constants of uniform distributions of aligned gas-filled (dry) and liquid-filled cracks of small aspect ratio. These formulations have been used by Crampin (1984) and others to model, apparently satisfactorily, the velocity- and attenuation-anisotropy of seismic waves propagating through EDA cracks in the crust. Note however, that these formulations have not been verified experimentally, although it has been established experimentally that shear-wave splitting does occur in both sedimentary (Rai & Hanson 1988) and igneous (Nur & Simmons 1969) rock samples subject to uniaxial compressional stress. The detailed matching of synthetic seismograms to observed waveforms in VSP experiments (Bush & Crampin 1987) suggests that the theoretical formulations are at least approximately correct.

Nishizawa (1982) also used Eshelby's (1957) technique to develop a general iterative procedure for determining the effects on seismic waves of scattering caused by distributions of elipsoidal inclusions for aspect ratios ranging from very small (flat cracks), through unity (spherical bubbles), to very large (needle-shaped inclusions). Hudson's formulations are valid for cracks of small dimensions relative to seismic wavelengths and for relatively weak distributions of cracks (CD $\leq$ 0.1, that is differential shear-wave anisotropy $\leq$10 per cent, say, where crack density CD = $N\bar{a}^3/v$ and N is the number of cracks of radius a in volume v). Nishizawa claims his formulations are valid for strong crack distributions.

With these limitations, the first- and second-order velocity variations are insensitive to the dimensions of the inclusions. The attenuation caused by scattering is more sensitive to crack dimensions (Hudson 1981). However, since the dimensions of EDA cracks are expected to range from perhaps a few microns in igneous and metamorphic rocks to submillimetre in sedimentary rocks, while the seismic wavelengths are of the order of tens of hundreds of metres, the effects on attenuation caused by scattering are likely to be small and will not be discussed here. Nishizawa's formulation does not model attenuation.

Douma (1988) compared Nishizawa's iterative procedure for small aspect ratios cracks with the algebraic formulations of Hudson (1980, 1981), and found the two procedures gave similar results for cracks with crack density CD $\leq$ 0.05 and aspect ratios up to $AR = d/a = 0.3$, where d is the half thickness and a is the radius of the cracks. In this paper, Douma's program (Douma 1988) is used to calculate Nishizawa's procedure for the effects of distributions of oblate spheroids (bubbles) with aspect ratios greater than or equal to 0.2. Hudson's formulations, following Crampin (1984), are used to calculate the effects of flat cracks with aspect ratios less than 0.2.

This paper discusses the effects of three types of uniform distributions of EDA cracks that could cause the shear-wave splitting observed in the crust (Crampin 1987): aligned flattened bubbles; parallel cracks; and aligned mixtures of bubbles and cracks (there may be two distinct populations of crack shapes in some rocks).

The Appendix shows the variations of waves through a fourth (simple) uniform distribution that can produce transverse isotropy: aligned elongated spheroids with aspect ratios greater than one. Such inclusions sometimes occur, possibly as an intermeidate stage, in the healing of flat cracks in igneous and metamorphic rocks (Smith & Evans 1984), but this is unlikely; the Appendix is included for completeness. Note that elongated spheroids would lead to the polarizations of the leading split shear waves being aligned parallel to the direction of the maximum compressional stress within the shear-wave window, similar to those through parallel vertical cracks, as is observed in the Earth's crust (Crampin 1987).

3 PROPAGATION THROUGH INCLUSIONS RANGING FROM SPHERICAL BUBBLES TO FLAT CRACKS

3.1 Variations in the plane perpendicular to the crack face

Figure 1 shows the velocity variations of seismic waves propagating through water-filled inclusions with aspect ratios ranging from AR = 1.0 (spherical bubbles) to AR = 0.001 (flat cracks) at three crack densities (a) CD = 0.1, (b) 0.05, and (c) 0.01. The variations are shown over the same range of velocities so that the results may be easily 'compared. All inclusions are in an isotropic matrix rock. The minor axes of the bubbles, and the normals to the crack faces are taken to be parallel. Each system of cracks is transversely isotropic (possesses hexagonal symmetry) and is effectively anisotropic to seismic waves. Consequently, three ***plane waves*** with mutually perpendicular polarizations may radiate in all directions of ***phase-velocity*** propagation (Crampin 1981). In general, there may also be three (or more) rays travelling in all directions of ***group-velocity*** propagation along seismic rays with ***curved wavefronts,*** but in this case the polarizations of the split shear waves will not be strictly orthogonal (Crampin 1981, 1989).

These three waves are an approximately radially polarized quasi-longitudinal wave, qP, and two quasi-shear waves, qSP and qSR, polarized (P)arrallel and at (R)ight angles, respectively, to the plane through the crack normals. [Note that the qSR-wave is strictly polarized perpendicular to the ray path and the 'q' may be omitted, Crampin (1989).] The two shear waves can be easily distinguished in the velocity variations, as qSP has a cos 48 variation with angle from the symmetry axis, whereas qSR has a cos 28 variation. The velocity variations of the two split shear waves intersect [in line-singularities, Crampin (1989)]. The direction of this intersection changes with the aspect ratio, with the changes

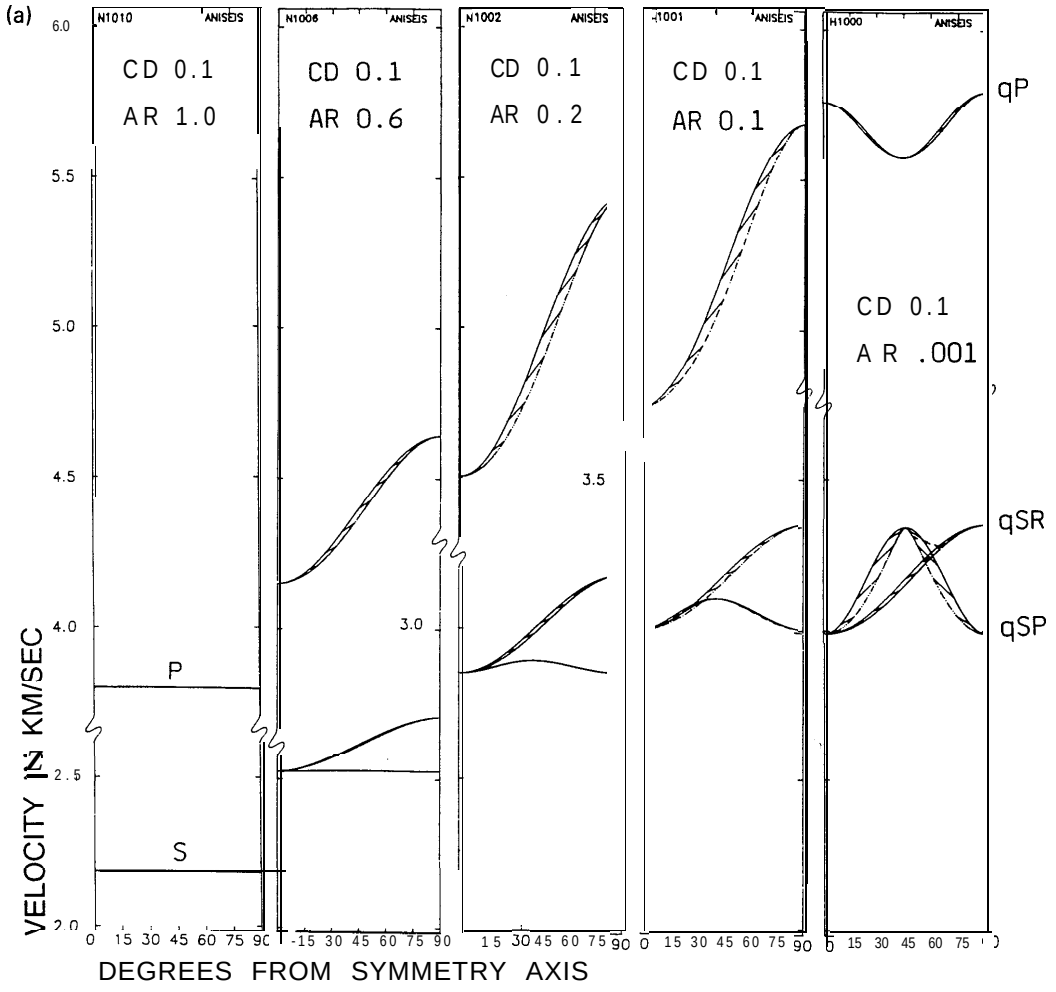

Fiire **1.** Variations of seismic body-wave velocities over a quadrant of directions through distributions of aligned water-filled inclusions with aspect ratios ranging from AR = 0.001 to AR = 1.0 at crack densities of (a) CD = 0.1, (b) CD = 0.05, and (c) CD = 0.01. The uncracked isotropic matrix material has velocities V_P = 5.8 and V_S = 3.349 km s^{-1} and density ρ = 2.6 g cm^{-3}. The liquid in the inclusions is water with velocity 1.5 km s^{-1}. The variations are shown over a quadrant of directions from parallel (0°) to perpendicular (90") to the axis of symmetry (crack normal or minor axis of spheroid). The solid upper line is the phase velocity and the broken lower line is the group velocity, which is joined to the appropriate phase velocity every 10° of phase velocity. The waves in (a) are labelled qP, for the approximately longitudinally polarized quasi-P-wave, and qSP and qSR, for the two quasi-shear waves polarized (P)arallel and at (R)ight angles to the plane through the symmetry axis. The *P*- and S-wave velocities in the isotropic structure (AR = 1.0) are labelled *P* and S, respectively.

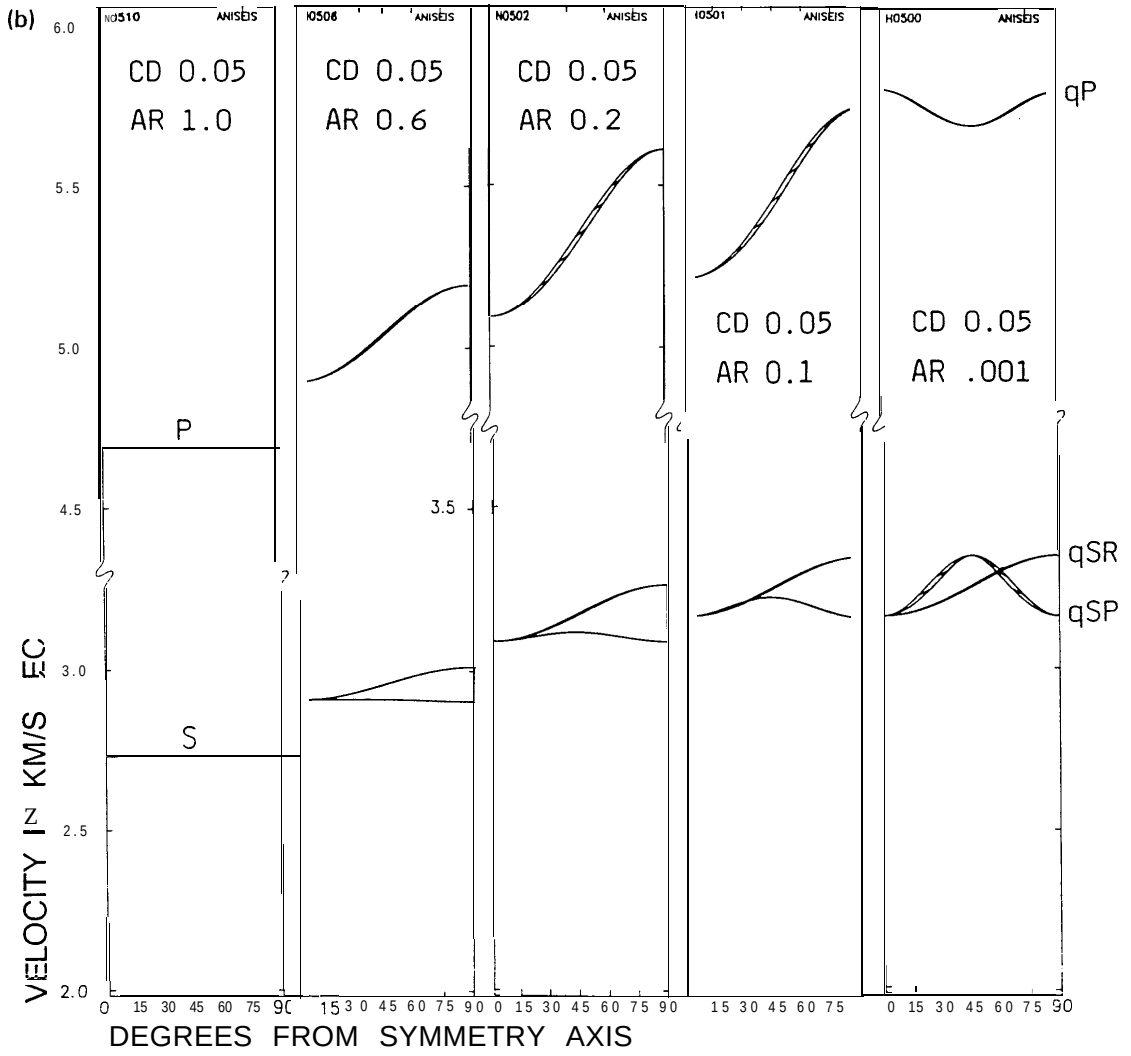

Figure 1. (continued)

being most marked at small aspect ratios. The planar variations at small aspect ratios are shown in more detail in Fig. 2 for a crack density of ***CD = 0.05.***

The crack densities of 0.1, 0.05, and 0.01 in Fig. 1 are equivalent to inclusions with diameters of 0.92, 0.74, and 0.44, respectively, in each unit cube. These crack densities yield differential shear-wave anisotropies for thin cracks which span those typically observed in sedimentary basins (Crampin *et al.* 1986b), and in igneous (Roberts & Crampin 1986) and metamorphic rocks (Crampin & Booth 1985) in the crust. Table 1 lists the percentages of anisotropy $[(V_{max} - V_{min}) \times 100/V_{max}$, Crampin (1989)] and porosity associated with the distributions of inclusions in Fig. 1. The porosities depend principally on the proportion of large aspect ratio cracks in the rock and again span those commonly observed in crustal rocks. It is worth noting that the velocities of the isotropic distributions of spheroidal inclusions (left-hand sides of Fig. la, b and c) also span the velocities of many particulate sedimentary rocks, such as sandstones. This suggests that a major component of the velocities in such rocks, for any given mineralogy, is determined by the scattering at the intergranular pore-space.

3.2 Effects on P-wave propagation

In general, the velocity of both qP- and qS-waves decreases as the aspect ratio, and hence porosity, increases at any given crack density without changing the average relative difference between the velocities-the Poisson's ratio of the isotropic distribution of spherical bubbles (AR = 1.0) is the same (σ = 0.25) as that of the uncracked rock matrix. As the aspect ratio increases, the amplitude of cos 2θ variation of the qP-wave velocity-anisotropy increases from being small for flat cracks (which have cos 48 variations), reaches a maximum at about AR = 0.2 with significant qP-wave velocity anisotropy, and then decreases to zero for distributions of spherical bubbles (AR = 1.0), when the rock is isotropic.

3.3 Effects on shear-wave propagation

In general, both the percentage of shear-wave velocity-ansiotropy and differential shear-wave ansiotropy decrease as the aspect ratio increases leading to isotropy for distributions of spherical bubbles. The two split shear waves, however, behave differently. The velocity-anisotropy

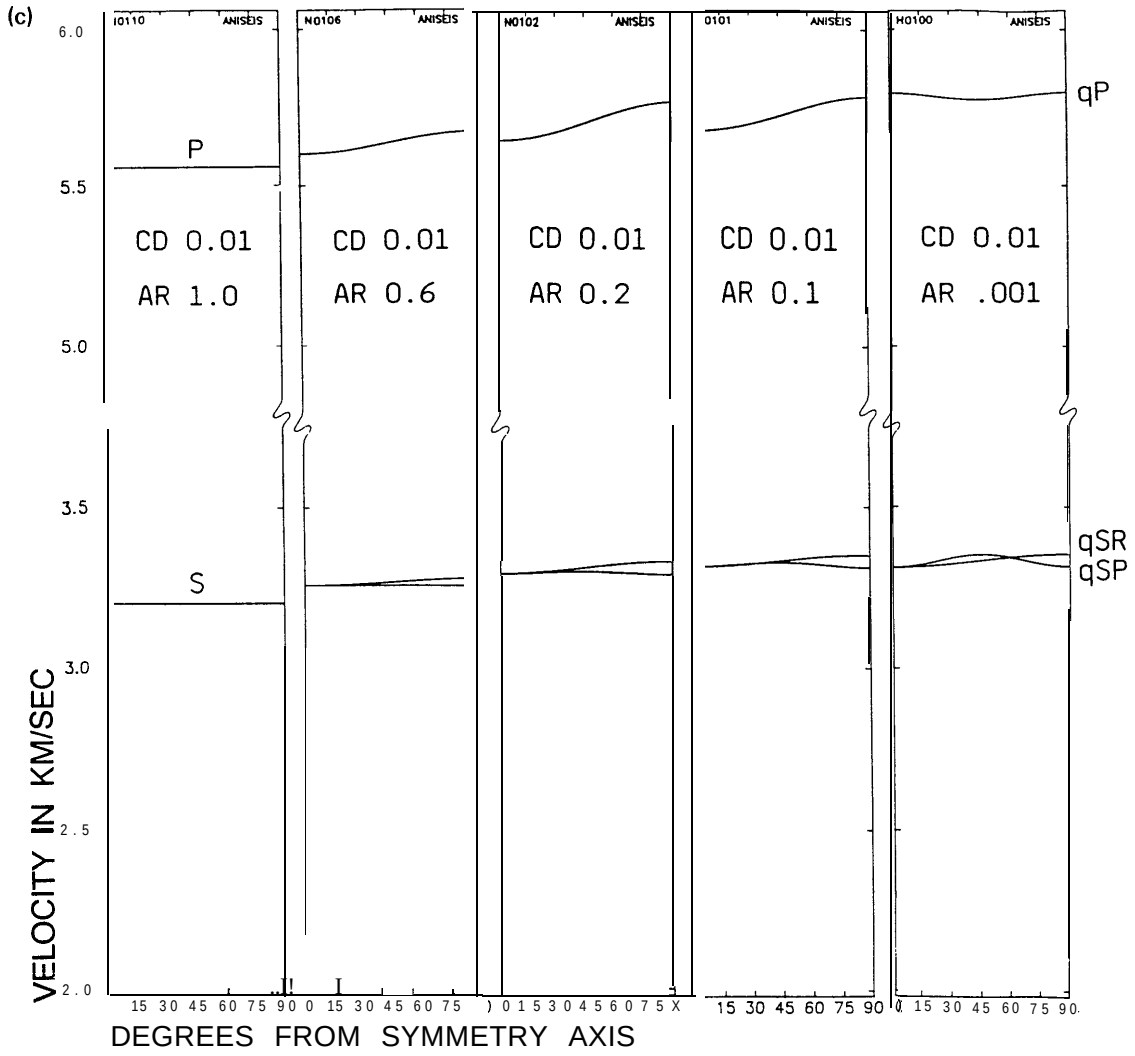

Fiie 1. (continued)

of the ***qSR*-wave,** polarized parallel to the crack face, decreases uniformly to zero as the aspect ratio increases to ***AR*** = 1.0, whereas the velocity-anisotropy of the ***qSP*-wave,** polarized at an angle to the crack face decreases more rapidly for small aspect ratios. (This is expected as the ***qSP*-wave** has particle displacements at an angle to the crack face and is more sensitive to the gap between the faces.) This means that the direction in which the shear-wave velocities intersect [in a line-singularity, **Crampin** (1989, **1991)]** moves towards the axis of symmetry as the aspect ratio increases. This is seen most clearly in Fig. 2. This movement is most rapid for small aspect ratios. The point of intersection moves from approximately 60" to the symmetry axis for flat cracks to coincident with the symmetry direction for all aspect ratios greater than about 0.2. Over the whole range of aspect ratios, the velocities of the two shear waves touch tangentially in the direction of the symmetry axis in kiss-singularities **(Crampin** 1989, **1991),** as they do for all transversely isotropic solids.

This behaviour of the shear-wave splitting is quite distinctive for variations of (small) aspect ratios, and variations in aspect ratio are inferred from the behaviour of shear-wave splitting before and after an ***M*** = 6 earthquake in California (Peacock et ***al.*** 1988; **Crampin** et ***al.*** 1990a) and before and after two small earthquakes in Arkansas (Booth et ***al.*** 1990). These temporal variations have been interpreted as the result of the elastic bowing (increase in aspect ratio) of fluid-filled **EDA** cracks as the stress builds up before the earthquake, followed by relaxation to flat cracks when the stress is released by the earthquake. Shear-wave splitting is sensitive to crack geometry. If the interpretation of these temporal changes in terms of varying aspect ratios is confirmed, it would suggest that it should be possible to monitor the detailed changes in reservoir rock during production and enhanced oil recovery operations by repeated shear-wave **VSPs.** (High-precision monitoring would require **VSPs** or cross-hole shooting to avoid the complexities associated with shear-wave interactions at the free **suface.)**

Note that for aspect ratios between about ***AR*** = 0.08 and 0.20, the velocities of the two split shear waves are tangentially close, and there will be no shear-wave splitting in a cone of directions about the symmetry direction. The cone has a half angle of about 35" for ***AR*** = 0.08 and progressively decreases to tangential contact in a **kiss-**singularity for aspect ratios less than about ***AR = 0.2.***

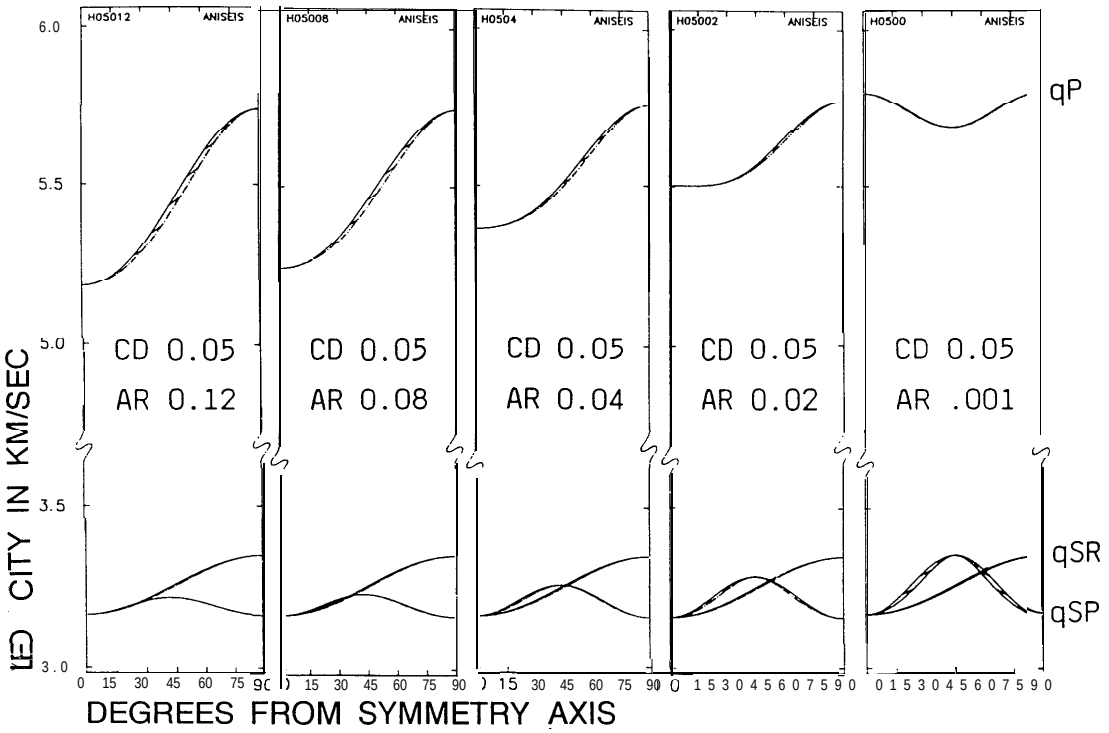

Figure 2. Variations in seismic body-wave velocities for aspect ratios of ***AR*** = 0.12 to ***AR*** = 0.001 for a crack density of CD = 0.05. Notation as in Fig. 1.

3.4 Variations in 3-D

Observations of shear-wave splitting in the crust appear to indicate that the inclusions in ***in situ*** rock are aligned vertically, striking perpendicular to the minimum horizontal compressional stress (Crampin 1987). Fig. 3 displays the 3-D variations of the group velocity of the split shear waves through a selection of the inclusions in Figs 1 and 2 in equal-area projections (polar maps) over a hemisphere directions. (The centre point of the projection represents a shear wave travelling vertically, and the edge of the projection represents a shear wave travelling horizontally at the appropriate azimuth.) The inclusions are aligned striking east-west with a north-south symmetry axis. The crack density is CD = 0.05 and aspect ratios range from ***AR*** = 0.001 to 0.6. The behaviour for aspect ratios between 0.6 and 1.0 is similar apart from a change in the delay between the split shear waves, and is not shown in Fig. 3. The left-hand side of Fig. 3 shows the horizontal polarizations of the leading (faster) split shear waves, ***qS1***, as seen by horizontal instruments, and the right-hand side shows the contoured time delays between the split shear waves ($t_{qS2} - t_{qS1}$) for a normalized path length. [Note that the notation for split shear waves is changed. The only unambiguous notation for split shear waves not propagating in a direction of sagittal symmetry is to distinguish between the faster (***qS1***) and slower (***qS2***) arrivals (Crampin 1989).] The inner circle in Fig. 3 marks the theoretical shear-wave window at a horizontal free surface for plane-wave propagation at an angle of incidence of 35°, for a Poissons's ratio of 0.25.

The direction in which the shear-wave velocities intersect (coincide) varies from approximately 60" from the symmetry axis for very small aspect ratios, to about 30" for an aspect ratio of ***AR*** = 0.1, and for ***AR*** greater than about 0.2 (see Fig. 1), the two velocities only touch tangentially in the direction of the symmetry axis. The effect on the 3-D behaviour is to broaden the band of parallel polarizations in Fig. 3 progressively with increasing aspect ratio until the polarizations of the first arrival are parallel for all directions of propagation for ***AR*** > 0.2. Thus, the polarizations of the

Table 1. Properties of the distributions of inclusions in Fig. 1.

Crack density (CD = $N a^3/v$)		Aspect ratio (AR = d/a) 1.0	0.6	0.2	0.1	<0.001
0.01	% P-wave anisotropy	0	1.2	2.0	1.9	0.40
	% diff.shear-wave anisotropy	0	0.70	1.2	1.1	1.1
	% porosity	4.2	2.5	0.84	0.42	<0.004
0.05	% P-wave anisotropy	0	5.9	9.3	9.2	1.8
	% diff.shear-wave anisotropy	0	3.4	5.3	5.5	5.6
	% porosity	21	13	4.2	2.1	<0.02
0.1	% P-wave anisotropy	0	11	17	17	3.0
	% diff.shear-wave anisotropy	0	6.6	10.2	10.7	10.7
	% porosity	41	25	a.4	4.2	<0.04

It is worth noting that, conveniently, the percentage of differential shear-wave anisotropy for thin cracks (AR ≤ 0.02) is approximately equal to the crack density times a hundred.

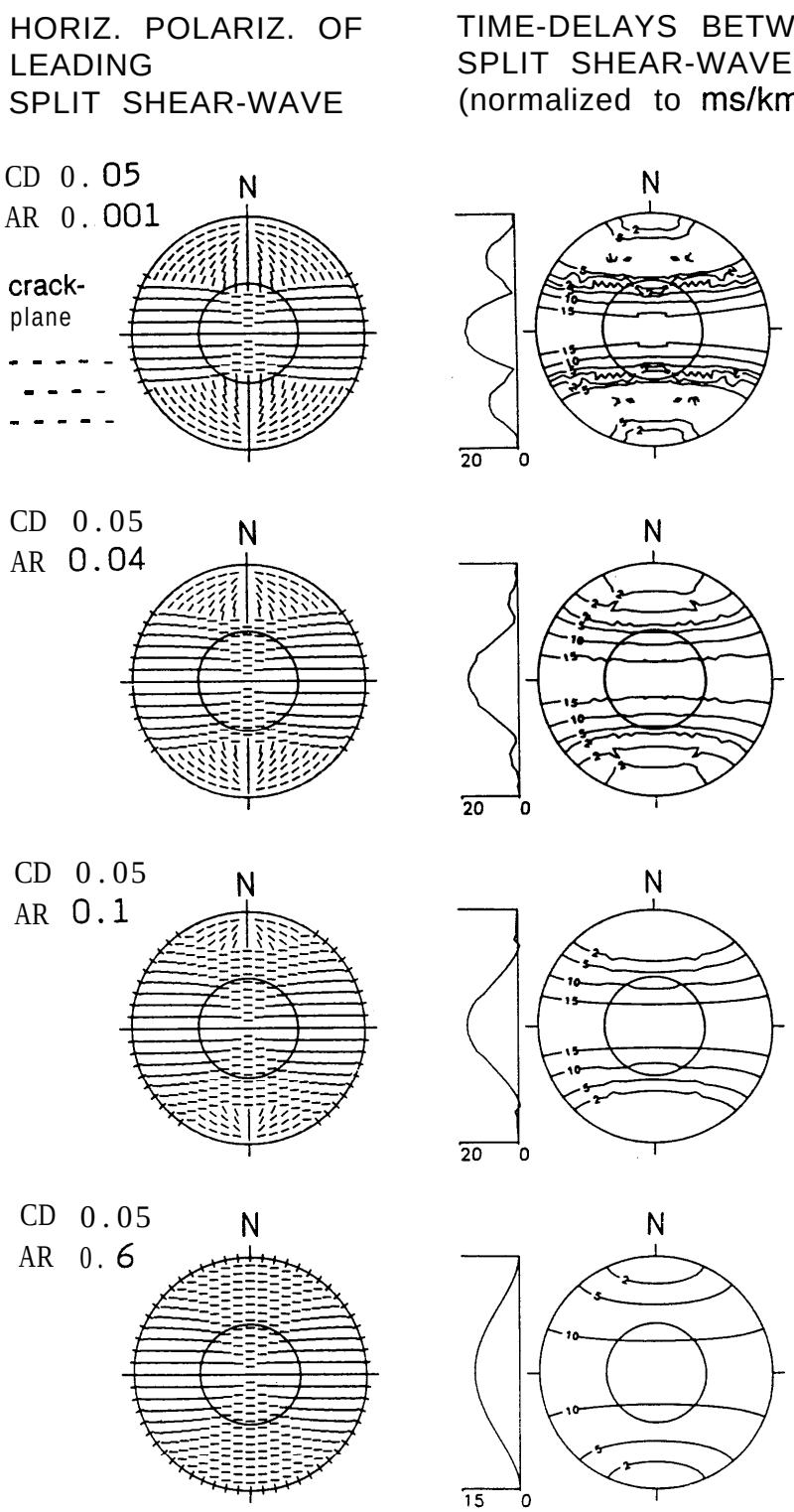

Figure 3. Equal-area projections over a hemisphere of directions of the 3-D pattern of behaviour of split shear waves propagating at the group velocity through a selection of the distributions of inclusions in Figs l(b) and 2, with the horizontal ases of symmetry north-south. The left-hand side shows polarizations of the leading (faster) split shear wave, ***qS1***, as recorded by horizontal seismometers, and the right-hand side shows the time delays between the split shear waves contoured in ms km-'. The irregularities in the contour lines are due to the complexities of group-velocity propagation (**Crampin** 1991). There is a north-south section of the delays to the left of the contoured projection.

leading split shear wave through thin parallel cracks are perpendicular to the axis of symmetry (and their horizontal projections are parallel to the strike of the cracks) only in a broad band across the centre of the projection, including almost the whole width of the shear-wave window. In contrast, the polarizations of the leading split shear waves propagating through flattened bubbles with $AR \geq 0.2$ *are* perpendicular to the axis of symmetry for all directions of propagation.

The velocity variations in Figs 1 and 3 are almost identical for the range of aspect ratios from about AR = 0.1 to about 0.2, for angles less than about 30" from the symmetry axis. Over this range of angles, the velocities are nearly coincident, and there is very little delay between the two shear waves, so that the shear waves radiated from the source will propagate unmodified by the anisotropy, except for, possibly, very high-frequency signals, or over very long paths. Note also that for distributions of inclusions with horizontal axes of symmetry, the situation believed common in the crust, these directions of negligible delays, which might be a distinctive and diagnostic characteristic, would be outside the shear wave window, and are unlikely to be observable along the nearly vertical ray paths in VSPs or reflection surveys.

4 MIXTURES OF OBLATE SPHEROIDS AND PARALLEL CRACKS

Shapes of fluid-filled inclusions probably vary with rock type. In igneous and metamorphic rocks it is likely that, in some circumstances, there exist two distinct populations of cracks: inter- and intragranular microcracks of small aspect ratio (Simmons & Richter 1976), and approximately spherical bubbles (Shepherd 1990). Inclusions may move from one population to another: microcracks may heal into strings or planes of bubbles; and bubbles under the action of stress may coalesce into cracks. These transitions are probably relatively rapid and, in general, the two populations may intermingle but each retain their separate identity. The bubbles are expected to be generally smaller than a few tens of microns.

Figure 4 shows the velocity variations of such mixtures of bubbles (AR = 0.8) and flat cracks with an overall crack density of CD = 0.05, where the symmetry axes (normal to the flattening) are parallel. [The two distributions of cracks were combined with the technique of Hudson (1986) correct to the second order of crack/crack interactions.] The qP-waves range from a small cos 2θ variation for oblate spheroids to a cos 48 variation for flat cracks, and the shear waves show behaviour intermediate to the unmixed behaviour at the sides of the figure. The behaviour of the qP-waves and the shear waves taken separately would be indistinguishable from the range of unmixed inclusions with the same crack density in Figs l(b) and 2. The mixture might be recognized only if accurate measurements of both qP-wave velocities and shear-wave splitting could be compared. Other examples (not shown) suggest that similar results hold for mixtures with different aspect ratios.

Inclusions in sedimentary rocks are likely to consist principally of intergranular pore-spaces. Such pores are likely to be severely irregular. Rock physics experiments demonstrate that under relatively large stress, these spaces

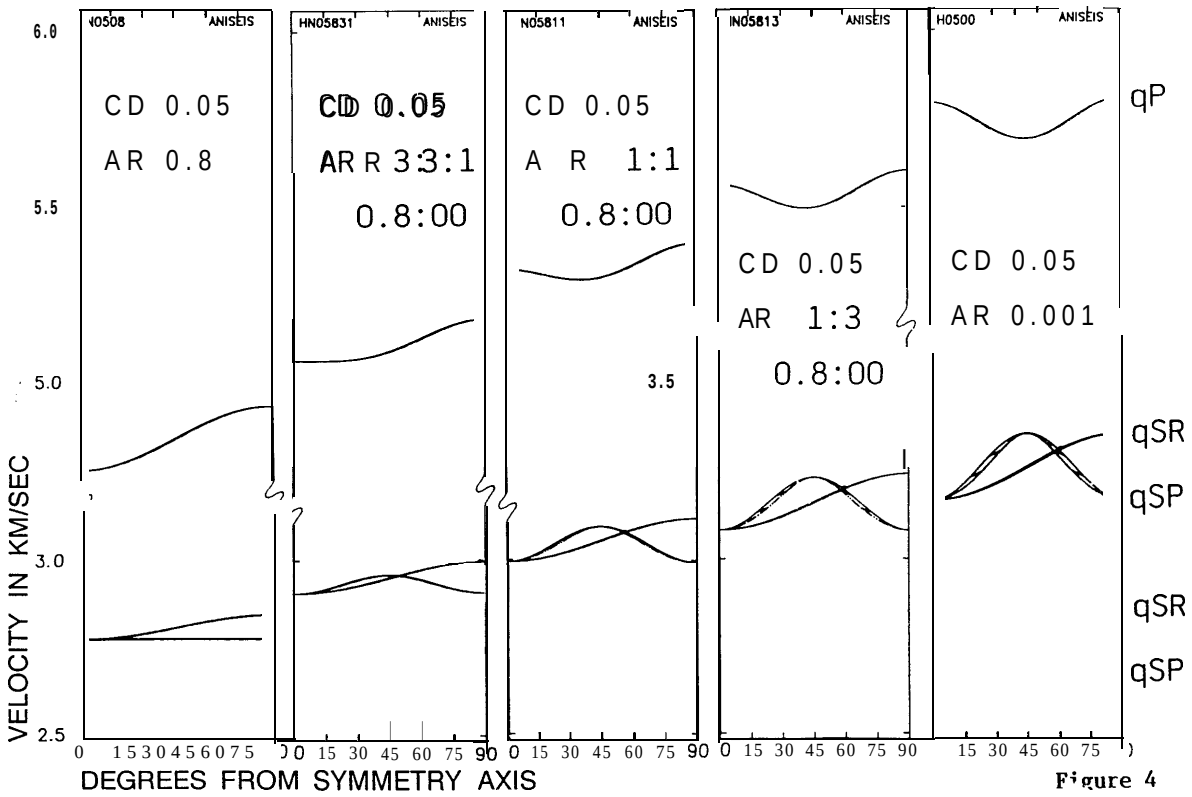

Figure 4

Fiire 4. Velocity variations in mixtures of liquid-filled oblate spheroids (AR = 0.8) and flat cracks (AR = 0.001) in the ratios 1:0, 3:1, 1:1, 1:3, and 0:1, respectively. Notation as in Fig. 1.

deform, and the rock is rendered effectively anisotropic (Rai & Hanson 1988). Similar deformation is expected under the possibly smaller but long-lasting regional deviatoric stress field in the crust by processes such as subcritical crack growth (Atkinson 1984). This would result in the shear wave splitting observed in sedimentary basins (Alford 1986; Willis, Rethford & Bielanski 1986; Crampin *et al.* 1986b) and in poorly consolidated sediments (Crampin *et al.* 1986a).

The widely observed shear-wave splitting suggests that the irregular pores in sedimentary rocks do display preferential stress-induced orientations (Crampin 1987). The inclusions are also likely to include another population of crack shapes of much smaller fluid-filled bubbles within each grain, although the porosity of these microinclusions is likely to be so much smaller than that of the intergranular pore space, that the seismic effects of this second population of micro-inclusions may well be negligible. Shear waves propagating through such rock would sample enormous numbers of inclusions per wavelength, and any estimate of the behaviour of shear waves would have to be based on average properties. It is likely that the average properties would be very similar to those in an appropriate mixture such as that illustrated in Fig. 4, which again are very similar to those in the range of single-shaped inclusions in Figs 1 and 2.

5 DISCUSSION

Table 2 summarizes some of the observed behaviour of shear wave splitting which may be relevant to the physical shape of fluid-filled inclusions that cause the anisotropy in the crust.

5.1 Polarizations of leading split shear wave generally parallel to direction of maximum compressional stress

This was one of the earliest characteristic features of shear wave splitting in the crust to be recognized (Crampin, Evans & Üçer 1985). There is frequently a scatter of up to $\pm 20°$ about the stress direction, which is almost certainly due to the interaction of shear waves with irregular surface topography. In areas, where there is smooth topography and no low-velocity surface layers, the polarizations show least scatter (Kaneshima, Ando & Crampin 1987). The scatter in surface observations appears to have two distributions: a scatter about the mean direction at each recording site, probably caused by local topographic or subsurface irregularities; and a scatter of the mean polarization at each recording site about the stress direction, probably related to the average dip of the topography. There may be systematic deviations from parallel polarizations in sedimentary basins as a result of the anisotropy being a combination of EDA anisotropy and the transverse isotropy of periodic, or subperiodic, thin layers (PTL anisotropy). This combination results in orthorhomibc symmetry which has several fundamental differences from hexagonal symmetry (Bush & Crampin 1987; Crampin 1988, 1989).

The fundamental feature of the generally observed parallel polarizations in the crust (for ray paths within 35" of the vertical) is reproduced in distributions of both flattened bubbles and thin cracks as long as the minor axes and crack

Table 2. Summary of observations of shear-wave splitting in the uppermost 10–20 km of the crust.

1) Polarizations of leading split shear-waves are generally parallel or subparallel to the direction of maximum compressional stress (Crampin 1987).
2) Maximum azimuthal differential shear-wave anisotropy are generally between 1% and 5% in sedimentary, metamorphic, and igneous rocks (Crampin 1987), although anisotropy of over 20% has been observed in specific structural elements (Bamford and Nunn 1977; Johnston 1986).
3) Temporal changes in shear-wave polarizations have been observed before and after hydraulic pumping (Crampin and Booth 1989).
4) Temporal changes in delays between split shear-waves have been observed before and after earthquakes (Peacock *et al.* 1988; Crampin *et* al. 1990; Booth et al. 1990).
5) Delays do not always get smaller towards the sides of the broad band of parallel polarizations, as expected from theoretical behaviour (Figure 3).

normals are parallel and horizontal (see Fig. 3). This is the orientation of industrial hydraulic fractures which, once below the immediate surface layers, are typically aligned vertical, striking perpendicular to the direction of minimum compressional stress, and hence parallel to the direction of maximum stress.

5.2 Maximum azimuthal differential shear-wave anisotropy of between 1 and 4 per cent

There are at present too few published values of azimuthal anisotropy to draw firm conclusions; however, there are observations of maximum values at both ends of the range of percentages in sedimentary rocks (4 per cent, Crampin *et al.* 1986a; l-3 per cent, Crampin *et al.* 1986b) and igneous rocks (1 per cent, Peacock *et al.* 1988; 4 per cent, Roberts & Crampin 1986), and several at about 4 per cent in metamorphic regimes (booth *et al.* 1985; Kaneshima *et al.* 1987). It is remarkable that despite the range of dimensions and types of inclusion expected in sedimentary, igneous, and metamorphic rocks the percentage of differential shear-wave anisotropy should be in such a narrow range.

These values can be exceeded in heavily fractured localities. Bamford & Nunn (1977) found up to 20 per cent P-wave anisotropy in shallow refraction experiments in limestone pavements, due to near-surface joints and fractures. This implies a differential shear-wave anisotropy of about 23 per cent (Crampin, McGonigle & Bamford 1980). Similarly, Johnston (1986) found a remarkable 27.5 per cent differential shear-wave anisotropy in the top few hundred feet of the Austin Chalk in the Marcelina Creek field, Texas. Some areas of the Austin Chalk is known to be heavily fractured, and this is presumably the cause of this high anisotropy.

5.3 Temporal changes in shear-wave polarizations observed before hydraulic fracturing

Crampin & Booth (1989) report changes in the polarizations of the faster split shear waves before and after hydraulic fracturing in the Cambourne School of Mines hot dry rock experiment, 1982, Cornwall. The faster split shear waves were parallel to the measured directions of the local stress before pumping, and parallel to joints on surface outcrops after pumping. The difference is only between 5" and 10°, but appears to be outside the error limits. This was interpreted as the hydraulic pumping dilating incipient joints in the ***in situ*** granite (at a small angle to the stress direction) that were previously held closed and transparent to shear waves. Thus, before pumping, the shear waves were parallel to the stress-oriented EDA cracks, and parallel to the newly opened joints after pumping, where the newly opened hydraulic fractures had reoriented the EDA cracks. This indicates that the polarizations of EDA cracks are sensitive to the stress directions, so that changes in these directions can be monitored by shear-wave splitting.

5.4 Temporal changes in delays before and after earthquakes

Peacock *et al.* (1988) and Crampin *et al.* (1990a) report temporal changes in shear wave splitting at one of the stations of the Anza seismic network before and after the M = 6 North Palm Springs earthquake of July 8 1986. (The station, KNW, was the only recording site above sufficient small earthquakes to show the anomaly.) The effects could be simulated by the elastic 'bowing' (increasing aspect ratio) of EDA cracks as the stress builds up before the earthquake, and the 'thinning' (decrease of aspect ratio) as the stress relaxes following the earthquake. Booth *et al.* (1990) reported similar variations in shear-wave splitting before and after much smaller events ($M < 4$) above the Enola swarm, Arkansas, 1982. The data at Enola were sparse, but are consistent with the observations at Anza.

The form of the reported temporal variations suggests that the shape of the fluid-filled EDA cracks, in at least igneous and metamorphic rocks, can be simulated by thin parallel cracks. This is not necessarily expected in sedimentary rocks, although Rai & Hanson (1988) have shown that under uniaxial stress the behaviour of sandstone can be modelled by flat cracks parallel to the direction of stress.

[Note that Aster, Shearer & Berger (1990) have reported examining the data set, where Peacock *et al.* (1988) and Crampin *et al.* (1990a) find temporal variations, with an automatic technique in an attempt to get a more objective assessment of shear-wave splitting. They find no evidence for temporal variations, but Crampin *et al.* (1990b) have shown that the parameters derived from the automatic technique of Aster *et al.* do not correlate with any identifiable features of the seismic records, and conclude that the automatic technique as used by Aster *et al.* is neither objective or meaningful in assessing shear-wave splitting above small earthquakes.]

5.5 Delays not always getting smaller towards the edge of the shear-wave window, as expected theoretically for thin liquid-filled cracks

Delays do not generally decrease away from the plane of the cracks, as expected from Fig. 3. The only examples where this has been clearly seen happen to have been for ray paths in granite batholiths: above shallow events induced by hydraulic pumping in hot dry rock experiments in Cornwall (Roberts & Crampin 1986); and above seismic events beneath a batholith recorded at MYO in the Abuyama network in Japan (Kaneshima *et al.* 1987). The significance of these observations being confined to granite batholiths has not been identified, but may be because of the absence of significant low-velocity near-surface layers in granite, which usually disturb the shear-wave ray paths.

5.6 Connectivity (permeability)

The figures in this paper refer specifically to isolated fluid-filled inclusions. Although such isolated inclusions may be found in impermeable hard rocks, in porous sedimentary rocks, particularly in reservoir rocks of economic significance, the interconnectivity of inclusions is likely to be high, and this will modify the internal stress field and hence modify seismic wave propagation.

There are no published formulations for the elastic properties of rocks containing pores linked by fluid paths, and it is not clear how the effects would differ from those of

isolated inclusions modelled in this paper. There are two considerations which suggest that there may be no major differences between the effects of isolated and connected EDA cracks, although the actual elastic constants may differ in detail. The first is that the dimensions of inclusions are small, probably submillimetre or less, and any crack connections are also likely to be small. Since the wavelengths of seismic signals are tens to hundreds of metres, the statistical sampling is extraordinarily good, and it is possible, that the effects of small-scale connections will also be small. The second consideration is that permeability frequently also displays anisotropy, and thin parallel parallel connection channels are likely to behave as parallel cracks, and the effects might well be modelled by mixtures of oblate spheroids and thin parallel cracks as in Fig. 4: in which case the figures and discussions in this paper could still be largely correct.

6 CONCLUSIONS

(1) The behaviour of shear wave splitting is distinctively different in distributions of stress-aligned oblate spheroids (elliptical pores) and stress-aligned flat cracks. The differences are most marked for small variations of aspect ratio of flat cracks.

(2) Shear-wave splitting is sensitive to the details of the geometry of, particularly, small aspect-ratio cracks. Such variations appear to have been observed before and after one large and two small earthquakes, and before and after hydraulic fractures. This suggests that it may be possible to use repeated VSPs to monitor the internal crack geometry of reservoir rocks as hydrocarbon is depleted and monitor the progress ***in situ*** of enhanced oil recovery (EOR).

(3) Flat cracks have only small effect on the velocities of *qP*-waves. The principal effect of increasing aspect ratio is to introduce a marked velocity anisotropy of the *qP*-wave with a cos 28 variation with direction. This near-ellipticity of the *qP*-wave velocity variations rapidly reaches a maximum at about ***AZ?*** = 0.2, and then slowly decreases until the rock is isotropic at an aspect ratio of 1.0.

(4) The scattering due to homogeneous distributions of fluid-filled spheres causes (isotropic) reductions in seismic velocities in rock similar to the velocities in particulate rocks (such as sandstones) made up of grains of higher velocity material (such as quartzites).

(5) This paper demonstrates that the previous analyses of shear-wave splitting on propagation through distributions of small aspect-ratio cracks can be consistently extended to distributions of oblate spheroids. There are many similarities in behaviour, but there are some distinguishing features that may be recognized by their effect on shear wave splitting.

ACKNOWLEDGMENTS

I thank Dr Jan Douma for allowing me to use his program for calculating Nishizawa's formulation, and Drs David C. Booth and Colin D. MacBeth for their comments on the manuscript. I also thank Don Winterstein for a very detailed review of the manuscript. The work was partially supported by the Edinburgh Anisotropy Project and the Natural Environment Research Council, and is published with the approval of the Director of the British Geological Survey (NERC).

REFERENCES

Alford, R. M., 1986. Shear data in the presence of azimuthal anisotropy: Dilley, Texas, ***Expanded Abstracts, S&h Ann. Int. SEG Mtg, Houston,*** pp. 476-479.

Aster, R. C., Shearer, P. M. & Berger, J., 1990. Quantitative measurements of shear wave polarizations at the Anza seismic network, Southern California-implications for shear wave splitting and earthquake prediction, ***J. geophys. Res., 95,*** 12 449-12 473.

Atkinson, B. K., 1984. Subcritical crack growth in geological materials, ***J. geophys. Res., 89,*** 4077–4114.

Bamford, D. & Nunn, K. R., 1977. ***In situ*** seismic measurements of crack anisotropy in the carboniferous limestone of Northwest England, ***Geophys. Prosp.,*** **27,** 322–338.

Booth, D. C., Crampin, S., Evans, R. & Roberts, G., 1985. Shear wave polarizations near the North Anatolian Fault-I. Evidence for anisotropy-induced shear-wave splitting, ***Geophys. J. R. astr. Soc., 83,*** 61-73.

Booth, D. C., Crampin, S., Lovell, J. H. & Chiu, J.-M., 1990. Temporal changes in shear wave splitting during an earthquake swarm in Arkansas, ***J. geophys. Res.,*** 95, 11151-11164.

Bush, I. & Crampin, S., 1987. Observations of EDA and PTL anisotropy in shear-wave VSPs, ***Expanded Abstracts, 57th Ann. Int. SEG Mtg, New Orleans,*** pp. 646-649.

Crampin, S., 1981. A review of wave motion in anisotropic and cracked elastic-media, ***Wave Motion, 3,*** 343-391.

Crampin, S., 1984. Effective elastic-constants for wave propagation through cracked solids, ***Geophys. J. R. astr. Soc., 76,*** 135-145.

Crampin, S., 1985. Evaluation of anisotropy by shear-wave splitting, ***Geophysics,*** **50,** 142-152.

Crampin, S., 1987. Geological and industrial implications of extensive-dilatancy ansiotropy, ***Nature,*** **328,** 491–496.

Crampin, S., 1988. Non-parallel shear-wave polarizations in sedimentary basins, ***Expanded Abstracts, 5&h Ann. Int. SEG Mtg, Anaheim,*** vol. 2, pp. 1130-1132.

Crampin, S., 1989. Suggestions for a consistent terminology for seismic ansiotropy, ***Geophys. Prosp, 37, 753-770.***

Crampin, S., 1990. Alignment of near-surface inclusions and appropriate crack geometries for geothermal hot-dry-rock experiments, ***Geophys. Prosp., 38,*** 621-631.

Crampin, S., 1991. Effects of singularities on shear wave propagation in sedimentary basins, ***Geophys. J. Int.,*** submitted.

Crampin, S. & Booth, D. C., 1985. Shear-wave polarizations near the North Anatolian Fault-II. Interpretation in terms of crack-induced anisotropy, ***Geophys. J. R. astr. Soc., 83, 75-92.***

Crampin, S. & Booth, D. C., 1989. Shear wave splitting showing hydraulic dilatation of pre-existing joints in granite, ***Sci. Drill.,*** 1, 21-26.

Crampin, S., Evans, R. & Atkinson, B. K., 1984. Earthquake prediction: a new physical basis, ***Geophys. J. R. astr. Soc., 76,*** 147-156.

Crampin, S., Evans, R. & Üçer, S. B., 1985. Analysis of records of local earthquakes: the Turkish Dilatancy Projects (TDP1 and TDP2), ***Geophys. J. R. astr. Soc., 83,*** 1-16.

Crampin, S., McGonigle, R. & Bamford, D., 1980. Estimating crack parameters from observations of P-wave velocity anisotropy, ***Geophysics, 45, 345-360.***

Crampin, S., Booth, D. C., Evans, R., Peacock, S. & Fletcher, J. B., 1990a. Changes in shear-wave splitting at Anza near the time of the North Palm Springs earthquake, ***J. geophys. Res.,*** 95, 11197-11212.

Crampin, S., Booth, D. C., Evans, R., Peacock, S. & Fletcher, J. B., 1990b. Response to comments by Aster ***et al.*** (1990) about

temporal variations in shear wave splitting observed by Peacock *et al.* (1990) and Crampin *et al.* (1990), *J. geophys. Res.,* in press.

Crampin, S., Booth, D. C., Krasnova, M. A., Chesnokov, E. M., Maximov, A. B. & Tarasov, N. T., 1986a. Shear wave polarizations in the Peter the First Range indicating crack-induced ansiotropy in a thrust-fault regime, ***Geophys. J. R. astr. Soc.,* 84,** 401–412.

Crampin, S., Bush, I., Naville, C. & Taylor, D. B., 1986b. Estimating the internal structure of reservoirs with shear wave VSPs, ***Leading Edge, 5,*** 11, 35-39.

Douma, J., 1988. The effect of the aspect ratio on crack-induced anisotropy, ***Geophys. Prosp., 36,*** 614-632.

Douma, J. & Crampin, S., 1990. The effect of changing aspect ratio of aligned cracks on shear wave VSPs: a theoretical study, ***J. geophys. Res., 95,*** 11293-11300.

Eshelby, J. D., 1957. The determination of the elastic field of an ellipsoidal inclusion, and related problems, ***Proc. R. Soc. Lond.,*** A, **241,** 376–396.

Fyfe, W. S., Price, N. J. & Thompson, A. B., 1978. ***Fluids in the Earth's crust, Developments in Geochemistry,*** vol. 1, Elsevier, Amsterdam.

Hubbert, M. K. & Willis, D. G., 1957. Mechanics of hydraulic fracturing, ***Trans. AZMME,* 210,** 153-170.

Hudson, J. A., 1980. Overall properties of a cracked solid, ***Math. Proc. Camb. phil. Soc., 88,*** 371-384.

Hudson, J. A., 1981. Wave speeds and attenuation of elastic waves in material containing cracks, ***Geophys. J. R. astr. Soc., 64,*** 133-150.

Hudson, J. A., 1986. A higher order approximation to the wave propagation constants for a cracked solid, ***Geophys. J. R. astr. Soc.,*** 87, 265-274.

Johnston, D. H., 1986. VSP detection of fracture-induced velocity anisotropy, ***Expanded Abstracts, 56th Ann. Int. SEG Mtg, Houston,*** pp. 464-468.

Kaneshima, S., Ando, M. & Crampin, S., 1987. Shear-wave splitting above small earthquakes in the Kinki District of Japan, ***Phys. Earth. planet. Inter., 45, 45-58.***

Nishizawa, O., 1982. Seismic velocity anisotropy in a medium containing oriented cracks—transversely isotropic case, ***J. phys. Earth, 30,*** 331-347.

Nur, A. & Simmons, G., 1969. Stress-induced velocity anisotropy in rock: An experimental study, ***J. geophys. Res., 74, 6667-6674.***

Peacock, S., Crampin, S., Booth, D. C. & Fletcher, J. B., 1988. Shear-wave splitting in the Anza seismic gap, Southern California: temporal variations as possible precursors, ***J. geophys. Res., 93, 3339-3356.***

Rai, C. S. & Hanson, K. E., 1988. Shear-wave velocity anisotropy in sedimentary rocks: a laboratory study, ***Geophysics,* 53,** 800-806.

Roberts, G. & Crampin, S., 1986. Shear-wave polarizations in a Hot-Dry-Rock geothermal reservoir: anisotropic effects of fractures, ***Int. J. Rock Mech. Min. Sci. Geomech. Abst.,* 23,** 291-302.

Shepherd, T. J., 1990. Fluid inclusions: the geological link between fluid-filled microcracks and shear-wave anisotropy, ***J. geophys. Res.,*** 95, 11 115-11 120.

Simmons, G. & Richter, D., 1976. Microcracks in rocks, in ***Physics and Chemistry of Rocks,*** pp. 105-137, ed. Strens, R. G. J., John Wiley and Sons, New York.

Smith, D. L. & Evans, B., 1984. Diffusional crack healing in quartz, ***J. geophys. Res., 89,*** 4125-4135.

Willis, H. A., Rethford, G. L. & Bielanski, E., 1986. Azimuthal anisotropy: occurrence and effect on shear wave quality, ***Expanded Abstracts, 56th Ann. Int. SEG Mtg, Houston,*** pp. 479-481.

APPENDIX : WAVE PROPAGATION THROUGH ELONGATED SPHEROIDS

Figure Al shows velocity variations and equal-area projections of polarizations and delays for shear waves propagating through distributions of elongated spheroids. The crack density is CD = 0.1 and the aspect ratio ***AR*** = 2.0. There are two distinct differences from the behaviour of oblate spheroids: the P-wave velocity variation shows a 180" phase difference, having a maximum value parallel to the symmetry axis, instead of a minimum; and the polarization of the leading split shear wave is parallel instead of perpendicular to the symmetry axis, but still parallel to. the direction of maximum stress. Increasing the aspect ratio, so that the inclusions become more needle-like, increases the velocity-anisotropy of the P-wave, and increases the delay between the split shear waves, but the general pattern of variations in Fig. Al persists.

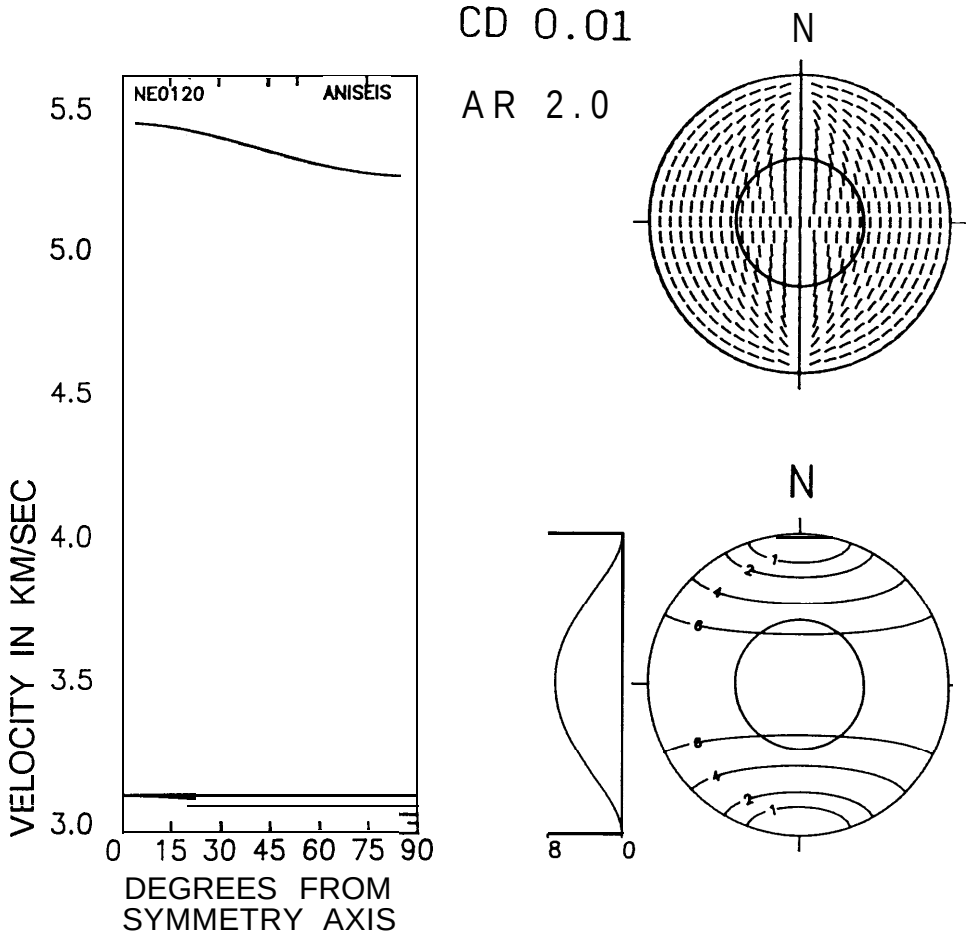

Figure A1. Velocity variations and equal-area projections for seismic waves propagating through distributions of elongated liquid-filled spheroids of crack density CD = 0.01 and aspect ratio ***AR*** = 2.0 in the same isotropic matrix as Fig. 1. Notation as in Figs 1 and 3.